Antenna-on-chip and antenna-in-package solutions to highly-integrated millimeter-wave devices for wireless communications

Zhang, Yue Ping; Liu, Duixian

2009

Zhang, Y. P., & Liu, D. (2009). Antenna-on-chip and antenna-in-package solutions to highly-integrated millimeter-wave devices for wireless communications. IEEE Transactions On Antennas And Propagation, 57(10), 2830-2841.

https://hdl.handle.net/10356/91623

https://doi.org/10.1109/TAP.2009.2029295

Antenna-on-Chip and Antenna-in-Package Solutions to Highly Integrated Millimeter-Wave Devices for Wireless Communications

Y. P. Zhang and Duixian Liu, *Senior Member, IEEE*

Invited Paper

***Abstract*—Antenna-on-chip (AoC) and antenna-in-package (AiP) solutions are studied for highly integrated millimeter-wave (mmWave) devices in wireless communications. First, the background, regulations, standard, and applications of 60-GHz wireless communications are briefly introduced. Then, highly integrated 60-GHz radios are overviewed as a basis for the link budget analysis to derive the antenna gain requirement. Next, in order to have deep physical insight into the AoC solution, the silicon substrate's high permittivity and low resistivity effects on the AoC efficiency are examined. It is shown that the AoC solution has low efficiency, less than 12% due to large ohmic losses and surface waves, which requires the development of techniques to improve the AoC efficiency. After that, the AiP solution and associated challenges such as how to realize low-loss interconnection between the chip and antenna are addressed. It is shown that wire-bonding interconnects, although inferior to the flip-chip, are still feasible in the 60-GHz band if proper compensation schemes are utilized. An example of the AiP solution in a low-temperature cofired ceramic (LTCC) process is presented in the 60-GHz band showing an efficiency better than 90%. A major concern with both AoC and AiP solutions is electromagnetic interference (EMI), which is also discussed. Finally, the systems level pros and cons of both AoC and AiP solutions are highlighted from the electrical and economic perspectives for system designers.**

***Index Terms*—60-GHz, antennas, liquid crystal polymer (LCP), low temperature cofired ceramic (LTCC) .**

I. Introduction

THE millimeter-wave (mmWave) frequency spectrum is defined to be 30 to 300 GHz, which corresponds to wavelengths from 10 to 1 mm. In this paper, however, we will focus specifically on the 60-GHz band (unless otherwise specified, the terms 60-GHz and mmWave are interchangeable). The history of mmWave technology began with the Indian physicist J. C. Bose who, in 1895 publicly demonstrated wireless signaling at frequencies as high as 60-GHz with various, now commonplace, microwave components including horn antennas [1]. Since then, no major work at 60-GHz had been reported until 1947 when the American physicist J. H. Van Vleck observed that the oxygen molecule absorbs electromagnetic energy more significantly at 60-GHz than at other frequencies [2]. The exploration of this phenomenon of nature was mainly driven by military and space applications during the 1960s to 1980s [3]. Starting from the late 1980s to the early 1990s, microcellular communication was the major driver. The microcell concept tried to use the higher path loss and oxygen absorption to intentionally limit 60-GHz link distance and allow for higher frequency reuse to increase the network capacity [4]. In the mid-1990s, interest in fixed broadband wireless access for last mile connectivity advanced 60-GHz radio technology [5]. Meanwhile, it was also realized that unlicensed use could be an appropriate regime for using such spectrum, since most of the justifications for radio licensing were not applicable in these frequencies [6].

As we entered the new millennium, Japan first issued 60-GHz regulations for unlicensed utilization in the 59–66 GHz band in the year of 2000. The maximum transmit power is limited to 10 dBm with maximum allowable antenna gain of 47 dBi and the maximum transmission bandwidth of 2.5 GHz [7]. In 2004, the United States allocated 7 GHz from 57–64 GHz for unlicensed use and specified the total maximum transmit power of 500 mW for an emission bandwidth greater than 100 MHz [8]. It should be mentioned that the 60-GHz regulation in Canada is harmonized with the US [9]. The 60-GHz regulation in Australia is, however, different from 7-GHz bandwidth allocated in Japan and North America. A narrower 3.5-GHz bandwidth from 59.4–62.9 GHz is allocated and the maximum transmit power is limited to 10 dBm [10]. In Europe, a wider 9-GHz bandwidth from 57–66 GHz is recommended with the maximum transmit power of 20 mW, maximum allowable antenna gain of 37 dBi, and the minimum transmission bandwidth of 500 MHz [11]. Table I lists the issued and proposed frequency allocations and radiation regulations for 60-GHz radios in a number of countries [7]–[13]. It should be mentioned that the maximum transmit power is also limited to 10 mW in the US and Canada when the electromagnetic radiation safety issues are considered.

Manuscript received June 29, 2008; revised December 04, 2008. First published August 04, 2009; current version published October 07, 2009.

Y. P. Zhang is with the Micro Radio Group, Division of Circuits and Systems, School of Electrical and Electronic Engineering, Nanyang Technological University, Singapore 639798, Singapore (e-mail: eypzhang@ntu.edu.sg).

D. Liu is with the IBM T. J. Watson Research Center, Yorktown Heights, NY 10598 USA.

Color versions of one or more of the figures in this paper are available online at http://ieeexplore.ieee.org.

Digital Object Identifier 10.1109/TAP.2009.2029295

TABLE I
FREQUENCY BAND AND LIMITS ON TRANSMIT POWER AND ANTENNA GAIN

Countries	Frequency Band (GHz)	Maximum Tx Power (mW)	Maximum Antenna Gain (dBi)
Japan	59-66	10	47
USA	57-64	500	Not Specified (NS)
Canada	57-64	500	NS
Australia	59.4-62.9	10	NS
Europe	57-66	20	37
China	57-66	10	NS
Korea	57-64	10	NS

TABLE II
IEEE 802.15.3C MODULATION SCHEMES

Transmission Mode	Schemes
Common Mode	$\pi/2$-BPSK
SC: Low Rate	$\pi/2$-BPSK
SC: Medium Rate	$\pi/2$-QPSK
	$\pi/2$-8QAM
SC: High Rate	$\pi/2$-QPSK
	$\pi/2$-16QAM
OFDM: Low Rate	QPSK
OFDM: Medium Rate	16QAM
OFDM: High Rate	64QAM

The IEEE 802.15.3c Task Group was formed in March 2005 to standardize 60-GHz radios. In July 2008, the Task Group is expected to finalize the standard [14]. To encompass available but inconsistent unlicensed frequencies, the draft standard divides nearly 9 GHz of spectrum from 57.24–65.88 GHz into four 2.16-GHz channels. The Nyquist bandwidth of the standard is 1.632 GHz with a guard bandwidth of 264 MHz on each side to prevent spectral leakage. The draft standard also enforces three basic transmission modes: common mode, single carrier (SC) mode, and the orthogonal frequency division multiplexing (OFDM) Mode. The Common Mode is used for channel scanning as well as low-speed communication with a $\pi/2$-binary phase shift keying $(\pi/2 - \mathrm{BPSK})$ at the base rate of approximately 50 Mb/s; while the SC and OFDM Modes are used for high-speed communication at the varied rates. The mandatory low rate required in both SC and OFDM Modes will be 1.5 Gb/s. Table II lists the modulation schemes in the standard [14]. It is seen that quadrature phase shift keying (QPSK) and quadrature amplitude modulation (QAM) are preferred.

A number of applications such as uncompressed high definition video streaming, mobile distributed computing, wireless gaming, Internet access, fast large file transfer, etc., are envisioned and detailed in the 802.15.3c usage model document [15]. This has attracted both large consumer electronics and small start-up companies to explore this space. To what extent and in what capacity these applications will be utilized will be determined by the ability of these companies to overcome 60-GHz technical challenges [16]. These challenges can be broadly classified into four categories: characterization of propagation channels, antenna technology, transceiver integration, and digital signal processing [17]. However, as will become clear in the next section, antenna technology affects radio propagation channels, transceiver designs, and choices of digital modulation schemes and hinders the establishment and reliability of a 60-GHz link. We will therefore concentrate on antenna technology and address newly proposed AoC and AiP solutions to highly integrated 60-GHz radios in this paper.

The remainder of this paper is organized as follows: Section II reviews the development of 60-GHz radio technology with an emphasis on the link budget analysis to derive the requirements for the antennas. Section III describes the AoC solution and techniques to improve the AoC performance. Section IV discusses the AiP solution and the associated challenges. Section V addresses electromagnetic interference. Finally, Section VI concludes the paper with highlights on the system level pros and cons of both AoC and AiP solutions from the electrical and economic perspectives.

II. 60-GHz RADIO ANTENNA TECHNOLOGY

In this section, highly integrated 60-GHz radios are overviewed as a basis for the link budget analysis to derive the antenna gain requirement.

A. Highly Integrated 60-GHz Radios

Traditional commercialized 60-GHz radios have been designed as an assembly of several microwave monolithic integrated circuits (MMICs) in gallium arsenide (GaAs) semiconductor technology. They have been used for Gigabit Ethernet (1.25 Gb/s) bridges between local area networks [18]. Recently, highly integrated transmitter (Tx) and receiver (Rx) MMICs in 0.15-μm GaAs pHEMT and mHEMT processes have been realized [19], [20]. The single-chip MMICs are especially well suited for transmission and reception of 60-GHz signals at data rates of several Gb/s [20]. However, the 60-GHz radios in GaAs MMICs have minimal integration and are expensive. In order for 60-GHz radios to have mass deployment and meet consumer marketplace requirements, the cost and size of any solution must be low-cost and compact. That implies silicon, not GaAs as the better technology choice. In fact, designs towards low-cost highly integrated 60-GHz radios have been realized in silicon technologies. For example, Floyd *et al.* have demonstrated a 60-GHz fully integrated radio transmitter and receiver chipset in a 0.13-μm silicon-germanium (SiGe) technology [21] and Wang *et al.* the 60-GHz fully integrated transmitter in a 0.18-μm SiGe technology [22]. Today, bulk CMOS at 130- and 90-nm nodes are capable of reasonable power gain at 60-GHz [23]–[29]. For example, Razavi has demonstrated a 60-GHz radio transceiver chip in a 0.13-μm CMOS [23] and Pinel *et al.* a 60-GHz transceiver chip in a 90-nm CMOS [26]. Building block circuits in a 65-nm CMOS have also been designed and characterized [30]. Table III gives some data of highly integrated 60-GHz radio chips in various semiconductor technologies from the open literature [19]–[29]. It is interesting to note that more chipsets are designed in CMOS and many of them utilize differential circuits. The noise figure (NF) of the receiver gets improved, but the output power of transmitter becomes inadequate as CMOS scales.

B. 60-GHz Radio Antenna Gain Requirement

The link budget for highly integrated 60-GHz radios is rather limited due to low transmit power (10 mW), large propagation loss (68 dB @ 1 m), and high data rate $(\geq 2\,\mathrm{Gb/s})$. Hence, the

TABLE III
DATA OF 60-GHz RADIO CHIPS

Technology	Die size (mm^2)	Bandwidth (GHz)	Circuit-to -antenna	Tx Power (dBm)	Rx Gain (dB)	Rx NF (dB)	Reference
0.15-μm GaAs pHEMT	5.0 × 3.5 (Tx)	54.0-61.0	Single-ended	3.3			[19]
	5.7 × 5.0 (Rx)	55.0-63.0	Single-ended		8.5	9.8	
0.15-μm GaAs mHEMT	4.0 × 3.0 (Tx)	56.5-64.5	Single-ended	5.6			[20]
	5.5 × 4.0 (Rx)	54.5-64.5	Single-ended		12.9	7.2	
0.13-μm SiGe BiCMOS	4.0 × 1.6 (Tx)	59.0-64.0	Differential	15-17			[21]
	3.4 × 1.7 (Rx)	59.0-64.0	Single-ended		38-40	5-6.7	
0.18-μm SiGe BiCMOS	1.3 × 0.8	58.0-62.0	Differential	15.8	N/A	N/A	[22]
0.13-μm CMOS	1.0 × 0.4 (Tx)	NA	Differential	-10			[23]
	0.3 × 0.4 (Rx)	NA	Single-ended		27.5	12.5	
0.13-μm CMOS	0.022	58.5-61.5	Differential	N/A	23.5	10.5	[24]
90-nm CMOS	2.4 × 1.1	61.34-63.4	Differential	N/A	22	8.2	[25]
90-nm CMOS	1.8 × 1.5(Tx)	57.0-64.0	Single-ended	5.1			[26]
	2.3 × 1.7 (Rx)	57.0-64.0	Single-ended		51	9	
90-nm CMOS	0.6 × 0.48	58.5-60.5	Single-ended	N/A	21	7.4	[27]
90-nm CMOS	0.5 × 0.37	57-61	Single-ended	N/A	18-22	5.7-8.8	[28]
90-nm CMOS	1.53	50-75	Single-ended	N/A	60	6.2	[29]

use of directional antennas is necessary, especially for line-of-sight (LOS) applications. The directional antennas reduce multipath effect and therefore simplify the design of 60-GHz radios. However, the directional antennas increase the outrage probability of the 60-GHz radios due to highly dynamic shadowing [31], [32]. Assuming that the gain values of both transmit and receive antennas are G_t and G_r, respectively, one can express their combination from the link budget equation as:

$$G_t + G_r = M + \frac{C}{N} + L_I + kT + 10\log B + NF + P_L + 10n\log d + X_\sigma - P_t \quad (1)$$

where M represents the link margin, C/N the carrier-to-noise ratio required for demodulation, L_I the implementation loss of a transceiver, k Boltzmann's constant, T the temperature, B the bandwidth, P_L the reference path loss at $d = 1\,\mathrm{m}$, n the loss exponent, and X_σ a zero mean Gaussian distributed random variable with a standard deviation σ, and P_t the transmit power. Unless otherwise specified, the parameters in (1) are $M = 10$ dB [17], $L_I = 6$ dB [33], $kT = -174$ dBm at a standard temperature 17 °C, $B = 2.16$ GHz, $NF = 7$ dB (a reasonable assumption based on Table III for Si technologies), $P_L = 68$ dB, $n = 2$ and $X_\sigma = 2$ dB for a LOS path in a typical indoor office [32], and $P_t = 10$ dBm. Therefore, (1) can be simplified as

$$G_t + G_r = 2 + \frac{C}{N} + 20\log d \quad (2)$$

for the LOS path. Now, it is clear that for the 60-GHz radio to cover a distance d, the combined antenna gain depends on C/N. The minimum C/N values for quasi-error-free reception by the $3/4$ coded OFDM system with guard interval $1/4$ in Rayleigh channels are 10.7 dB for QPSK, 16.7 dB for 16-QAM, and 21.7 dB for 64-QAM, respectively [32]. Table IV shows the combined antenna gains in dBi required for the LOS path calculated from (2). Taking the case of QPSK with the data rate of 2 Gb/s at $d = 10\,\mathrm{m}$ as an example, one can see that the combined antenna gain required for the LOS path is 33 dBi.

TABLE IV
COMBINED ANTENNA GAIN REQUIRED FOR THE LOS PATH

Distance (m)	QPSK (2 Gbps)	16-QAM (4 Gbps)	64-QAM (6 Gbps)
1	13	19	24
5	27	33	38
10	33	39	44
20	39	45	50

C. 60-GHz Antenna Technology

Typical antenna types for mmWave radio systems are reflector, lens, and horn antennas. Reflector antenna technology has achieved the highest level of development for high gain applications. Lens antennas are a second in high gain technology; while horn antennas limit gain to about 30 dBi due to construction capabilities [34]. Although these types of antennas have high gain, they are not suitable for commercial (consumer) 60-GHz radios because they are expensive, bulky, heavy, and more importantly they can not be integrated with solid-state devices. Thus, one has to turn to printed antenna arrays for mmWave radio systems. Printed antenna arrays such as microstrip patch or dipole arrays have many unique and attractive properties—low in profile, light in weight, compact and conformable in structure, and easy to fabricate and integrate with solid-state devices. Hence, they are suitable for commercial 60-GHz radios and efforts are now being undertaken for mass production [35].

Fig. 1 shows the calculated gain levels of microstrip antenna arrays based on a typical substrate material with relative permittivity $\varepsilon_r = 2.15$ and loss tangent $\tan\delta = 0.001$ in the 60-GHz band as a function of number of elements for both center- and edge-fed cases. The microstrip antenna arrays consist of $2^n \times 2^n$ elements ($n = 1, 2, 3\ldots$) with an inter-element distance of half a free space wavelength 2.5 mm. The size of each element is determined to be 2 mm × 1.5 mm by the cavity model. Obviously, the required combined antenna gain is achievable for the specified modulation scheme at the targeted data rate for the LOS path with such an array. However, it becomes difficult to achieve for the NLOS path, which is usually caused by human

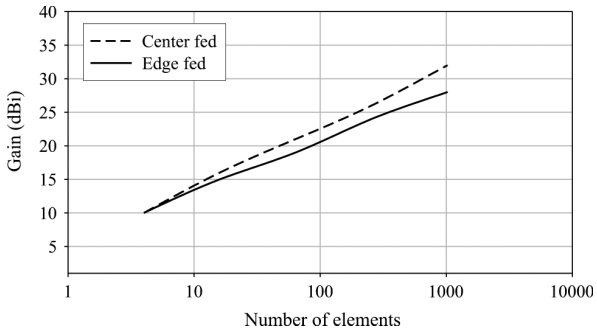

Fig. 1. Achievable gain of microstrip antenna arrays of $2^n \times 2^n$ elements in the 60-GHz band.

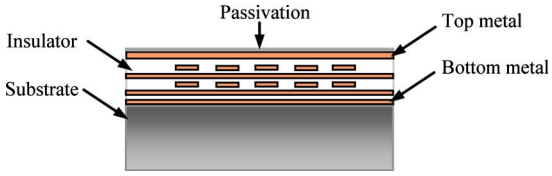

Fig. 2. Illustration of the cross section of silicon chip.

blockage. Experiments show that the effect of human blockage varies from 18-36 dB at 60-GHz in indoor environments [36]. If this happened, the combined antenna gain could become prohibitively high. To overcome such a problem, a switched-beam or adaptive antenna array is required to search and beamform to the available path. Switched beam arrays can be implemented more easily than adaptive arrays. Switched beam arrays select from a set of fixed beams to cover a given area; while adaptive arrays require the capability of continuously adjusting phase shift among the array elements. Adaptive antenna arrays are thought to be a key technology for 60-GHz radios, particularly for those implemented in CMOS [23].

Antennas and antenna arrays for highly integrated radios operating at 60-GHz or above have received great attention [37]–[40], especially the AoC and AiP solutions [22], [23], [25], [41]–[60]. This is not only because the antenna form factor at 60-GHz is on the order of millimeters or less, which opens up new integration options on a chip or in a package, but also obvious advantages of cost, compactness, reliability, and reproducibility of both AoC and AiP solutions. In the following Sections, we focus on these for 60-GHz radios.

III. AoC

The AoC solution features the integration of antennas or arrays together with other front-end circuits on the same chip in mainstream silicon technologies such as SiGe or CMOS. It should be mentioned that the AoC is not simply a matter of straightforward copy of integrated antennas developed in GaAs, for instance, vias-to-ground can be easily realized through the substrate in standard GaAs, but not in a standard silicon process. Fig. 2 shows the cross section of a silicon chip. Note that multiple metal layers are embedded between insulator layers on the substrate. In a standard silicon process, the thickness of metal layers ranges between 0.2 to 4 μm and the insulator layers between 0.2 to 1 μm. The number of metal layers is currently 6–8 and the separation from the top to bottom metal layers rarely exceeds 15 μm. The thickness of the substrate is typically 500–750 μm. The metal is either aluminum or copper. The insulator is SiO_2 or its variations with $\varepsilon_r = 2.2$–4. The substrate is silicon with $\varepsilon_r = 11.9$ and is doped to exhibit low resistivity $\rho = 10\ \Omega \cdot$cm, which is substantially smaller than that of GaAs substrates ($\rho = 10^7$-$10^9\ \Omega \cdot$cm).

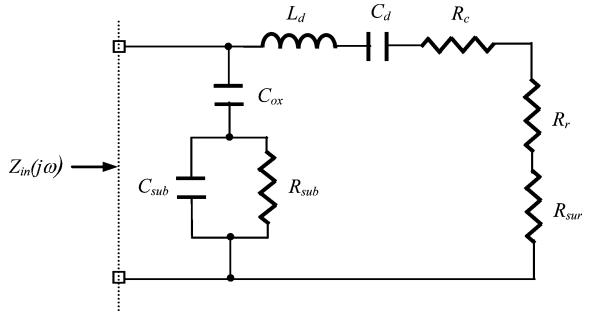

Fig. 3. Equivalent circuit model of an AoC with an off-chip ground shield.

The largest die size of the current 60-GHz radio in silicon, as shown in Table III, is about 6.4 mm^2. Considering the possibility of integrating more circuits such as the baseband processor on the same chip, one can expect that the die size may increase to tens of mm^2. Consequently, more area may be available to integrate more antenna elements in an array format. Nevertheless, we believe that high-directivity AoC is not practical at 60-GHz with the expected die size. The key parameters for the AoC thus become input impedance bandwidth and radiation efficiency [40].

Fig. 3 shows an AoC equivalent circuit model. In the model, the series branch comprises R_r, R_c, $R_{\rm sur}$, L_d, and C_d. Resistances R_r, R_c, and $R_{\rm sur}$ account for the radiation, conductor, and surface-wave losses of the AoC, respectively. L_d and C_d are the inductance and capacitance of the AoC, respectively. The shunt branch consists of $C_{\rm ox}$, $C_{\rm sub}$, and $R_{\rm sub}$. $C_{\rm ox}$ represents the oxide capacitance between the AoC and the silicon substrate. $C_{\rm sub}$ and $R_{\rm sub}$ are the silicon substrate capacitance and resistance, respectively.

The input impedance of the AoC can be written from the equivalent circuit model as (3), shown below, where

$$R_d = R_c + R_r + R_{\rm sur} \tag{4}$$

$$Z_{\rm in}(j\omega) = \frac{\left[1 - \omega^2 \left(C_d C_s R_d R_s + C_d L_d\right)\right] + j\left\{\omega\left[C_d R_d + C_s R_s \left(1 - \omega^2 C_d L_d\right)\right]\right\}}{\left[-\omega^2 C_d C_s \left(R_d + R_s\right)\right] + j\left[\omega\left(C_d + C_s - \omega^2 C_d C_s L_d\right)\right]} \tag{3}$$

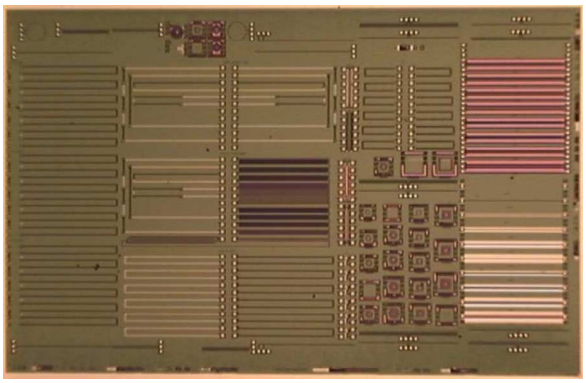

Fig. 4. Photograph of an AoC test vehicle.

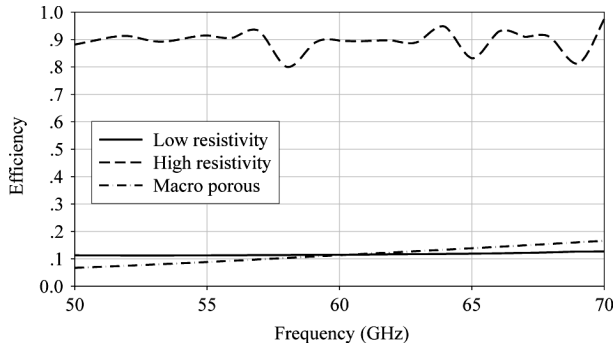

Fig. 5. Simulated AoC efficiency results with an off-chip ground shield.

$$R_s = \frac{R_P}{1+\omega^2 R_p^2 C_p^2} \tag{5}$$

and

$$C_s = C_p\left[1+\frac{1}{\omega^2 R_p^2 C_p^2}\right] \tag{6}$$

with

$$R_p = \frac{1+\omega^2 R_{\rm sub}^2 \left(C_{\rm sub}+C_{\rm ox}\right)^2}{\omega^2 R_{\rm sub} C_{\rm ox}^2} \tag{7}$$

and

$$C_p = \frac{\omega C_{\rm ox}+\omega^2 R_{\rm sub}^2 C_{\rm sub}\left(C_{\rm sub}+C_{\rm ox}\right)C_{\rm ox}}{1+\omega^2 R_{\rm sub}^2\left(C_{\rm sub}+C_{\rm ox}\right)^2}. \tag{8}$$

The radiation efficiency of the AoC can be expressed as

$$\eta = \frac{R_r}{{\rm Re}\left[Z_{\rm in}\left(j\omega_d\right)\right]} \tag{9}$$

where ${\rm Re}[Z_{\rm in}(j\omega_d)]$ is the real part of the input impedance of the AoC at the resonance angular frequency

$$\omega_d = \frac{1}{\sqrt{L_d C_d}}. \tag{10}$$

Note that $R_p \propto R_{\rm sub}$ from (7) and $R_s \propto 1/R_P$ from (5), this leads to

$$R_s \propto \frac{1}{R_{\rm sub}} \propto \frac{1}{\rho}. \tag{11}$$

It is found numerically from (9) that the silicon substrate of low resistivity results in poor radiation efficiency.

Dipole, monopole, inverted-F, Yagi, slot, and patch have been used in the AoC designs [22], [23], [25], [41]–[50]. Among them, dipole and Yagi are popular because they are differential and can be connected to differential circuits of highly integrated 60-GHz radios without using lossy baluns. Fig. 4 shows the die photograph of an AoC test vehicle. The dipole near the right edge is designed for the 60-GHz band.

Fig. 5 shows the HFSS simulated efficiency of an AoC with an off-chip ground shield. The AoC is an on-chip dipole that has an arm size of 1000 μm $\times$ 20 μm $\times$ 4 μm and is placed away from the edge of a die size of 5 mm $\times$ 5 mm $\times$ 0.5 mm by 100 μm. The AoC is assumed to be realized using the top metal (copper) supported by a 9 μm SiO_2 layer ($\varepsilon_r = 4$) on a 487 μm Si substrate of low resistivity $\rho = 10\ \Omega\cdot$cm. Note that the simulated efficiency of the AoC is poor, only 11.5% at 60 GHz. This is expected from the combined effect of the low resistivity and high permittivity of the silicon substrate. The low resistivity causes loss due to heating in the presence of an electric field in the substrate and the high permittivity causes loss due to power trapped in surface-wave modes in the substrate. To improve the AoC efficiency, it is important to know which is the major contributor to the poor AoC efficiency, the low resistivity or the high permittivity. Fig. 5 also shows the HFSS simulated AoC efficiency results for both high resistivity and macro porous Si, respectively. For the case of high resistivity Si, the resistivity is increased to $\rho = 10^3\ \Omega\cdot$cm; while for the case of macro porous Si, $\varepsilon_r = 2.2$ for the SiO_2 layer and $\varepsilon_r = 6$ for the Si substrate are assumed. It is evident from the figure that the low resistivity is the dominant factor to poor AoC efficiency [61].

Having understood the loss mechanisms, we now describe a few techniques to improve the AoC efficiency.

A. Substrate Thinning

A study of integrated microstrip dipoles in GaAs shows that optimum radiation efficiency can be obtained when the substrate thickness T is chosen at the cutoff thickness of the surface-wave TE_0 mode given by $\lambda_{\rm g}/4$ where $\lambda_{\rm g}$ is the guided wavelength in the substrate [62]. This choice is appropriate for GaAs, but not for silicon substrates because they have very low resistivity resulting in significant ohmic losses that cannot be neglected. A careful investigation of radiation and propagation mechanisms shows that the AoC efficiency can be improved by thinning silicon substrates. According to mode theory, substrate thinning to less than $\lambda_{\rm g}/4$ cuts off all surface-wave modes except TM_0. This mode contributes constructively to the directly radiated field through reflection at the ground plane and refraction at the substrate-air interface, thus improving the radiation efficiency.

The TM_0 surface-wave mode is an approximate plane wave because the E-field component is quite weak in the mode propagation direction. It undergoes large attenuation over the propagation in the substrate of low resistivity. To have a smaller attenuation, the substrate should be chosen much thinner than the thickness given by

$$T = \left[\omega\sqrt{\frac{\mu_r\mu_0\varepsilon_r\varepsilon_0}{2}}\left(\sqrt{1+\left(\frac{1}{\omega\rho\varepsilon_r\varepsilon_0}\right)}-1\right)\right]^{-1} \quad (12)$$

where the symbols have their usual meaning. As an example, consider a silicon substrate with $\varepsilon_r = 11.9$ and $\rho = 10\,\Omega\cdot$ cm, we find T to be 1.3 mm at 60 GHz. Choosing a thickness 5 times thinner than this value yields 260 μm, which happens to be around the wafer thickness, thinned before dicing. HFSS simulation shows that the efficiency of the AoC on a 241-μm Si substrate can be doubled to 23% at 60 GHz. Further thinning is possible, but more mechanical and reliability issues arise. In addition to substrate thinning, other approaches are available in a volume process such as placing the dipole nearest to the chip edge or furthest to the substrate which can also improve the AoC efficiency.

B. Proton Implantation

To avoid latch-up, low resistivity silicon substrates are preferred; while to improve mmWave antenna or other passive elements performance, high resistivity silicon substrates are favored. To solve this contradictory requirement of high and low substrate resistivity for single-chip mmWave radios, a proton implantation process has been developed to increase the resistivity of silicon substrates from $10\,\Omega\cdot$ cm to $10^6\,\Omega\cdot$ cm underneath selected devices [43]. The proton implantation uses the low energy proton implant of ~ 4 MeV after device fabrication, to avoid contamination of process integration and degradation to the gate oxide with radiation generated by nuclear reactions. Moreover, smaller implantation depth can be easily achieved by masking with commercial thick photoresists to enable the selective creation of high resistivity region below the desired devices such as antennas. A monopole fabricated using aluminum of 4 μm thick and 0.922 mm long on 1.5 μm oxide on silicon substrate of 525 μm thick was characterized comparatively with and without proton implantation. The measured results showed that the monopole gain with proton implantation was significantly higher than that without, for both average and peak gain values of 4.2 and 6.4 dB at 103 GHz, respectively.

C. Micromachining

Micromachining techniques use either wet or dry backside etching to selectively remove parts of the bulk silicon substrate. In the wet etching process, a silicon wafer is typically submerged in a chemical liquid to create cavities and membranes in the substrate. An advantage of wet etching is the batch type nature of the process, that is, several wafers can be submerged in the chemical liquid simultaneously, thus allowing low cost production. However, the etching is restricted by the crystal planes in the substrate, thus leaving the etched cavities with slanted walls. In the dry etching process, a single wafer is put in an evacuated chamber where plasma is generated to etch the silicon substrate. It is capable of yielding cavities with vertical walls, thus allowing substrate material to be selectively removed with good precision. A disadvantage of dry etching is generally it is more costly because of the expensive equipment used and time required [47].

A micromachining technique can be used to remove silicon substrate in areas where the AoC produces high field strength. This is important because it can not only reduce the substrate loss due to low resistivity and high permittivity so as to improve AoC efficiency, but can also reduce the problem of mechanical stability of the whole chip. One specific AoC design consists of two stacked high resistivity silicon substrates: 1) the top substrate of 254 μm thick, which carries the microstrip antenna, is micromachined with dry etching to create a 3 mm $\times$ 3 mm $\times$ 0.2 mm large cavity to improve the radiation performance of the AoC and 2) bottom substrate of 100 μm, which carries the microstrip feed line and the coupling slot. The measured return loss was more than 35 dB at 62-GHz. The measured impedance bandwidth was 6 GHz and simulated efficiency was 77% [47]. Another AoC has been designed and fabricated on a 1 μm quartz membrane on a $10\,\Omega\cdot$ cm silicon substrate of 550 μm thick by wet etching for the 60-GHz band [48]. Since the depth of the etched cavity is 400 μm and the silicon substrate underneath the antenna is still quite thick, comparison with the AoC on the non-micromachined substrate shows that radiation efficiency of the micromachined AoC has only been improved by a factor of 1.3.

D. Superstrate Focusing

It has been well known that by properly choosing superstrate, a significant improvement in directivity and efficiency of integrated antennas can be achieved, enabling the superstrate to act as a desirable part of the antenna as well as a protective layer [63]. The improvement in directivity can be explained as a focusing effect and as the suppression of surface-wave excitation. A cavity-backed slot-type AoC is implemented with the top and bottom metal layers on a silicon substrate with $\varepsilon_r = 11.9$ and $\rho = 10\,\Omega\cdot$cm. On top of the slot layer there is a superstrate layer of high permittivity that improves the radiation efficiency. The superstrate measures 1 mm $\times$ 0.25 mm $\times$ 0.6 mm and has the dielectric constant 38. The required silicon area for the implementation of 60-GHz antenna is 0.25 mm^2. The radiation efficiency of more than 30% is achieved [50]. It should be noted that superstrate focusing improves the AoC radiation performance at the cost of bandwidth. Also, the superstrate focusing technique should be developed as a part of standard packaging process to reduce the cost.

Improvement of the AoC radiation by using exotic techniques such as proton implementation and micromachining deviates from mainstream silicon technology, which undoubtedly increases the cost of the total solution. Nevertheless, the realization of a truly single-chip 60-GHz radio and avoidance of transmission loss due to interconnect are still encouraging circuit designers to explore the integration of an antenna (or antennas) with other circuits on a single-chip for very-short-range

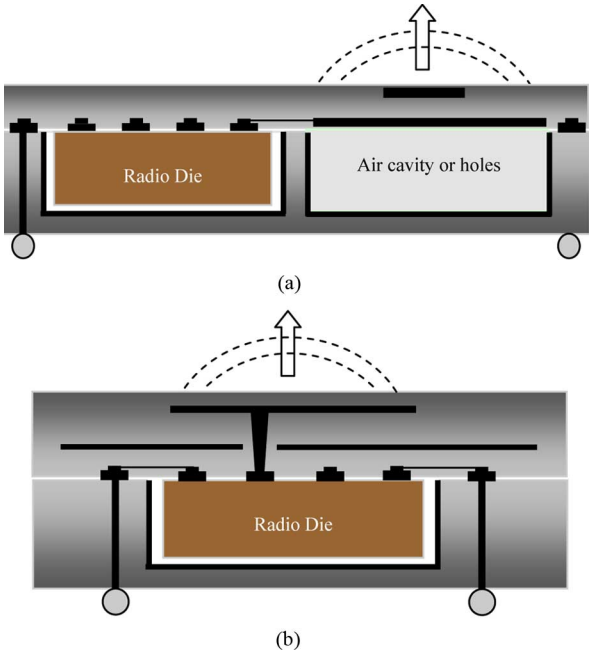

Fig. 6. Illustrations of AiP solution: (a) horizontal and (b) vertical configurations.

wireless communications or array applications [22], [23], [25], [35].

IV. AiP

The AiP solution combines an antenna (or antennas) with a highly integrated radio die into a standard surface mounted chip-scale package device, which is a recent innovative and important development in the miniaturization of wireless systems. The AiP solution has been recognized as the most promising antenna solution to highly integrated mmWave radios for high-speed short-range wireless communications because of high gain and broad bandwidth [50]–[60]. Fig. 6 illustrates two basic configurations of the AiP solution to highly integrated mmWave radio devices. For the first configuration shown in Fig. 6(a), two cavities are formed in the package. One houses the highly integrated radio die and the other, air-filled, enhances the antenna performance. For the second configuration shown in Fig. 6(b), the highly integrated radio die is packaged with the antenna on a multilayer structure in a vertical stacking configuration. Interconnection between the radio die and the antenna can be realized by using either wire-bonding or flip-chip techniques for the first configuration and by using the flip-chip technique for the second configuration. It should be emphasized that both wire-bonding and flip-chip techniques are inductive interconnections, which exhibit higher frequency bounds. Interconnection using the electromagnetic- or capacitive-coupling techniques directly between the radio die and the antenna for both configurations is also possible at even higher frequencies.

A. Materials and Technologies

Materials and process technologies capable of realizing AiP in high volume for mmWave radios are limited. Materials like high-resistivity silicon, Teflon, ceramics, polymers are candidates. Among them, low temperature cofired ceramic (LTCC) and liquid crystal polymer (LCP) materials and associated process technologies are particularly attractive [64].

There are several LTCC materials and processes in the market. To our knowledge, Ferro A6-S LTCC material is suitable for mmWave applications. It has been characterized over a frequency range up to 110 GHz showing $\varepsilon_r = 5.9 \pm 0.2$ and $\tan\delta < 0.002$ at 60, 77, and 94 GHz. Based on Ferro A6-S material, LTCC process technologies have been successfully developed in different foundries to realize functional packages [65], antennas [66], and AiP designs [67] for applications in the 60-GHz band. New advances in LTCC promise thinner ceramic types from standard 100 to 50 μm, finer line widths from typical 100 to 35 μm, and slimmer via diameters from 100 to 50 μm suitable for applications at even higher frequencies. As with any material, LTCC has limitations; for example, it laminates at temperatures above 850 °C, which is far above that which destroys active devices. So despite the ability to create hermetic multilayer substrates with integrated passive elements and antennas, the active devices must still be packaged separately and connected after the firing process [64].

Recently, LCP material has drawn much attention in the packaging industry because of its excellent mechanical, electrical and thermal characteristics. LCP process technologies have also been improving rapidly. Compared with LTCC, LCP has lower $\varepsilon_r = 3 \pm 0.2$ and slightly higher $\tan\delta = 0.002$-0.004 to the mmWave bands. Also, LCP has thinner thickness of 25 μm and finer line width and space of a few micrometers. More importantly, LCP has its ability to create near-hermetic homogeneous multilayer dielectric laminations at a temperature of 285 °C low enough to potentially package both active and passive devices into a compact module [64]. All these have generated great interest in using LCP for mmWave applications. It is therefore believed that LCP is well suited for mass production of AiP designs for 60-GHz radios.

B. Interconnection

Interconnection between the radio die and the antenna in the AiP solution should provide good return loss and low insertion loss over the signal frequency range. Two kinds of interconnect techniques are available in the mainstream packaging industry. They are the wire-bonding and flip-chip techniques [68]–[70]. Interconnection using the wire-bonding technique has been identified as one of key challenges because the discontinuity introduced by the bond wire can significantly affect the performance of the entire radio at mmWave frequency. Nonetheless, the wire-bonding technique, well established in consumer electronics, remains a very attractive solution since it is robust and inexpensive. In addition, it has the advantage of being tolerant on chip thermal expansion, an important requirement for many applications. Interconnection using the flip-chip technique has better performance than using the wire-bonding technique because the bump height is kept smaller than the length of the bond wire and the bump diameter is thicker than that of the bond wire. A bond wire as a series inductor will drastically increase the impedance and loss as the frequency or the length are increased. Hence, compensation is needed for the wire-bonding

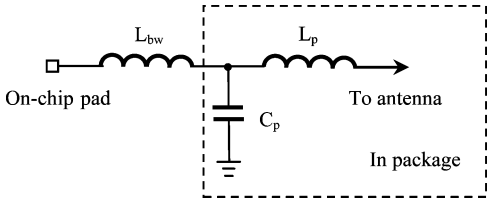

Fig. 7. Asymmetric compensation scheme in a T-Network.

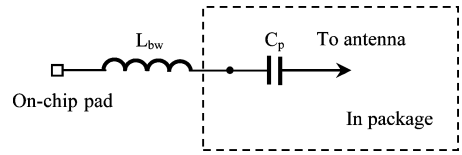

Fig. 8. Asymmetric compensation scheme in a series network.

technique. Symmetric compensation consumes additional die area and often results in output impedance different from the usual $50\ \Omega$ reference. Therefore, asymmetric compensation of only one terminal of the bond wire in the package is preferable in the AiP solution and many other cases.

Fig. 7 shows an asymmetric compensation scheme in a T-network for the bond wire. L_{bw} models the bond-wire inductance to be compensated by adding inductance L_p and capacitance C_p in the package. This scheme for a signal bond wire has been used in [40] and [71]. This scheme has two drawbacks: one is the large in-package area required to implement L_p and C_p and the other is the interconnect between the radio chip to the antenna requiring a DC blocking capacitor on the chip. Fig. 8 shows another asymmetric compensation scheme [72]. As shown, a series capacitance tunes the inductance of the bond wire to a resonant condition, thus compensating the high inductance of the bond wire at the resonant frequency. In the mmWave frequency range, the capacitance for the compensation is on the order of tens of femtofarads or less, making the structure very compact. In addition, it does not need to implement the DC blocking capacitor on the chip.

C. An AiP Example

IBM researchers have demonstrated a complete AiP solution for 60-GHz radios in a land grid array package using plastic mold injection technology and have shown that a folded dipole antenna suspended in a metal cavity has very good radiation efficiency about 90% [51]–[54]. Toshiba engineers have demonstrated another AiP solution, which connects the chip 60-GHz input and output pads to the metal plate on the chip mounting substrate with bonding wires to form a three-dimensional triangular loop. The three-dimensional triangular loop creates distance between the chip and the strong electric current, thereby minimizing deterioration of efficiency [55]. An AiP example based on Ferro A6-S LTCC is shown in Fig. 9 for highly integrated 60-GHz radios. The size of the whole AiP is $12.5 \times 8 \times 1.265\ \text{mm}^3$. Note the stepped cavity can house a highly integrated 60-GHz radio die of current size. The antenna consists of a slot radiator, a guard-ring director, a ground-plane reflector, and a fence of vias. A well-controlled electromagnetic environment is created for the antenna part of the AiP, which makes

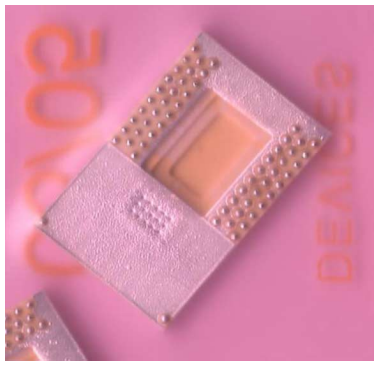

Fig. 9. Photograph of an AiP example.

the antenna performance less sensitive to the carried radio die, printed circuit board dielectric and metallic structures-an important design feature for system integration. The isosceles triangular slot with the base about one guided wavelength λg is inductively fed with a 50-Ω coplanar waveguide (CPW). The guard ring is about $\lambda g/2$ wide. The gaps between the guard ring and the slot radiator are smaller than $\lambda g/2$. The fence of vias shorts the outer metal edge of the slot radiator to the reflector. The ceramic material under the slot radiator is modulated with air holes to reduce surface waves. A quasi-cavity-backed slot antenna is thus realized in the package.

Fig. 10 shows the HFSS simulated and measured performance of the AiP. It is seen that they are in good agreement. The simulated and measured return loss values are higher than 7 dB from 59 to 65 GHz indicating acceptable matching to a 50-Ω source at these frequencies. The simulated and measured radiation patterns of the AiP at 61.5 GHz reveal that the H-plane patterns are similar too, but the E-plane patterns are different from those of a conventional cavity-backed slot antenna. A shaped-beam pattern can be seen in the co-polar E-plane with the main beam in the directions from 45° to 60°. The shaped-beam pattern in the co-polar E-plane is mainly caused by the package ground. The measured and calculated peak gain values for the slot AiP in the main beam direction are 11 and 9.5 dBi at 61.5 GHz, respectively with an estimated efficiency of 94%.

V. Electromagnetic Interference

A major concern with both AoC and AiP solutions is electromagnetic interference (EMI), which causes mutual coupling and affects the proper operation of the antenna and circuits. An understanding of the coupling mechanisms, impact of the process technology, grounding effects, guard rings, shielding, filtering, and decoupling is necessary to reduce EMI.

For the AoC solution, the circuits, especially their power lines, inductors, and capacitors will detune the antenna and affect its radiation patterns. Hence, the layout of the antenna should be kept away from them as far as possible [50]. On the other hand, the antenna couples to the circuits, especially the sensitive low noise amplifier, may degrade their performance. Two major coupling mechanisms are known, one is the substrate coupling and the other is the power-line coupling. The use of differential topology in the antenna and circuits can

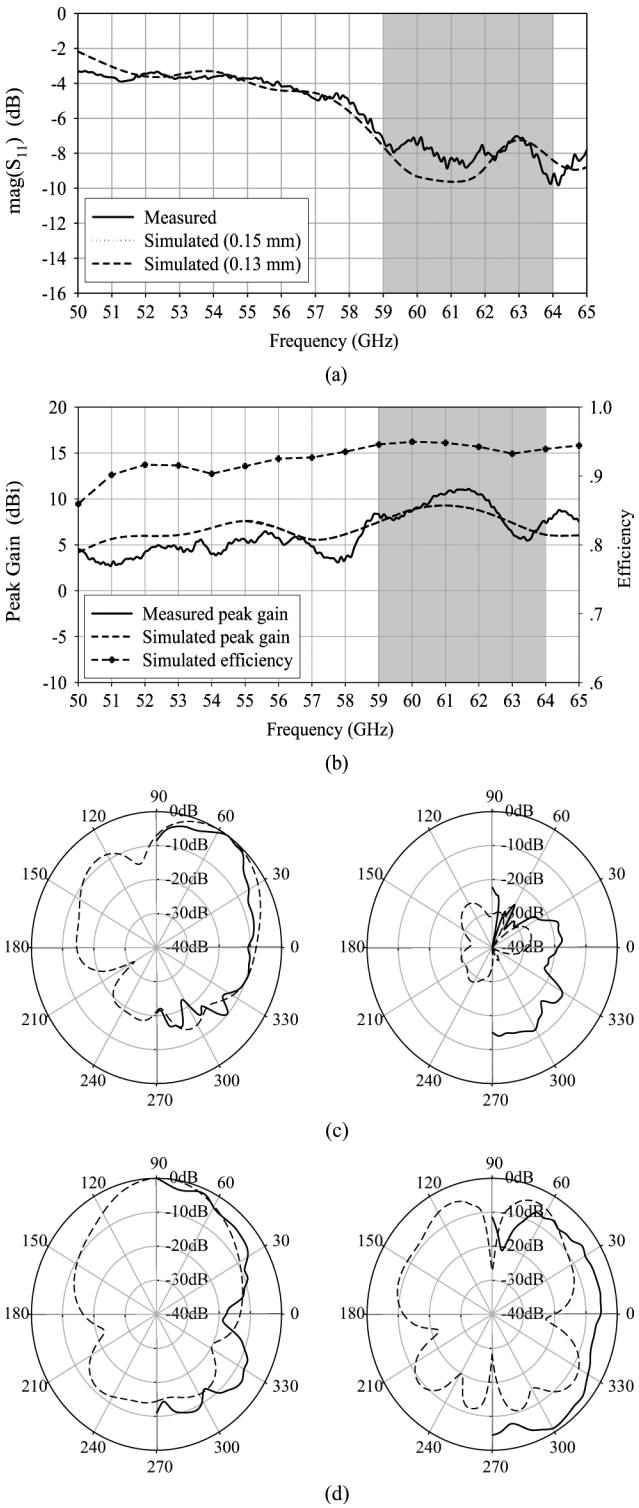

Fig. 10. Simulated and measured performance of the AiP: (a) magnitude of S_{11}, (b) gain and efficiency, (c) E-Plane patterns, and (d) H-Plane patterns.

substantially reduce EMI though the substrate coupling because the coupled crosstalk appears as common-mode in nature. The ability to suppress the substrate coupling also explains the popularity of dipole and Yagi in the AoC solution. The widespread of the power lines on the chip can be an unintended antenna [47] with which the AoC can couple. It is known that this coupling mechanism can be effectively prevented by using filtering and decoupling techniques implemented with the power lines.

For AiP solution, EMI is mainly generated from the discontinuity of interconnection between the chip and antenna, the excitation and propagation of surface waves, and the antenna far-field radiation. The techniques to reduce EMI are the use of differential antennas, air cavity and holes, guard rings, and fences of vias. The design guideline of the guard rings and fences of vias for the AiP solution using microstrip antennas can be found in [73].

VI. Conclusion

Driven by the release of the regulations in many countries, the imminent approval of the IEEE standard, and the potential of many exciting high-volume applications, one can see that a paradigm shift is taking place in the integration of mmWave 60-GHz radios from high cost and low volume in compound semiconductor technologies such as GaAs, towards low cost and high volume in silicon semiconductor technologies such as CMOS. Due to limited transmit power, high propagation loss, and data rate, the directional antenna plays a crucial role in these 60-GHz radios. The antenna gain requirement has been derived from the link budget analysis. Two antenna concepts known as the AoC and AiP solutions have received considerable attention recently. The AoC solution tries to realize the antenna (or antennas) on the same chip as other circuits in the mainstream semiconductor technology and the AiP solution manages to realize the antenna (or antennas) in the package that carries highly integrated mmWave radios in a packaging technology.

Virtually, all components including the antenna should be integrated on chip for reliability and cost reasons, but one has to admit that the silicon substrate is not optimized for antenna integration. The effects of the high permittivity and low resistivity of the silicon substrate limits the AoC efficiency to less than 12%. The techniques that can improve the AoC efficiency such as substrate thinning, proton implantation, micromachining, and superstrate focusing are either rather limited or deviate from the mainstream high volume processing techniques, which undoubtedly increases the cost and reduce the reliability of the whole system. Nevertheless, the realization of a truly single-chip 60-GHz radio, avoidance of transmission loss due to chip-to-package interconnect, and no need to use electrostatic discharge circuits are yet encouraging circuit designers to explore the integration of an antenna (or antennas) with other circuits on a single-chip for very-short-range wireless communications, arrays and sensor applications. The AiP solution is the most elegant and promising antenna solution to highly integrated mmWave radios for high-speed short-range wireless communications because of high gain and broad bandwidth. The major AiP challenge of how to realize low-loss interconnections between the chip and antenna has been addressed. It has been proven that the wire-bonding interconnect, although inferior to the flip-chip, is still feasible in the 60-GHz band with the proper compensation schemes. An example of the AiP solution has been given in LTCC showing high efficiency more than 90%. Both AoC and AiP solutions cause EMI issues. To reduce the negative effects due to EMI, the use of differential topology in the antenna and circuits is

suggested. Such techniques as shielding, guarding, filtering, and decoupling are effective to suppress EMI.

As the current AiP solution uses only one antenna element, the gain is not enough, so it is necessary to extend it to an antenna array to achieve gain of more than 25 dBi in LTCC. Also, the development of the AiP solution in LCP or at even higher frequency, say, 100 GHz is worthwhile. Furthermore, the codesign of mmWave radio in silicon with the antenna elements in the package to realize switched beam arrays or adaptive arrays appears more important. It is therefore anticipated that the works presented in this paper are useful and inspiring for those interested in the development of highly integrated mmWave radios for emerging high-speed short-range wireless communications.

ACKNOWLEDGMENT

The authors would like to thank Dr. M. Sun of Nanyang Technological University, Mr. K. M. Chua, and Ms. L. L. Wai of Singapore Institute of Manufacturing Technology for their contribution in the development of the LTCC-based AiP solution. The authors also thank the team at the IBM communication technology group at IBM T.J. Watson Research Center, Yorktown Heights, NY, and the IBM SiGe technology group at Burlington, Essex Junction, VT.

REFERENCES

[1] D. T. Emerson, "The work of Jagadis Chandra Bose: 100 years of mm-wave research," *IEEE Trans. Microw. Theory Tech.*, vol. 45, no. 12, pp. 2267–2273, Dec. 1997.

[2] J. H. Van Vleck, "The absorption of microwaves by oxygen," *Phys. Rev.*, vol. 71.7, pp. 413–424, 1947.

[3] A. R. Tharek and J. P. McGeeham, "Outdoor propagation measurements in the millimeter wave band at 60 GHz," *Proc. Military Microwaves*, vol. 88, pp. 43–48, Jul. 1988.

[4] S. W. Wales and D. C. Rickard, "Wideband propagation measurements of short range millimetric channels," *Electron. Commun. Eng. J.*, vol. 5, no. 4, pp. 249–254, Aug. 1993.

[5] [Online]. Available: http://www.proxim.com/products/landing_backhaul.html

[6] [Online]. Available: http://www.marcus-spectrum.com/MMW.htm

[7] Regulations for Enforcement of the Radio Law 6-4-2 Specified Low Power Radio Station (11) 59-66 Band. The Ministry of Public Management, Home Affairs, Posts and Telecommunications of Japan, 2000.

[8] Code of Federal Regulation, Title 47 Telecommunication, Chapter 1, Part 15.255. U.S. Federal Communication Commissions (FCC), 2004.

[9] Radio Standard Specification-210, Issue 6, Low-Power Licensed-Exempt Radio Communication Devices (All Frequency Bands): Category 1 Equipment. Industry Canada Spectrum Management and Telecommunications (IC-SMT), 2005.

[10] Radio Communications (Low Interference Potential Devices) Class License Variation 2005 (No. 1), The Australia Communications and Media Authority (ACMA), 2005.

[11] Electromagnetic Compatibility and Radio Spectrum Matters (ERM); System Reference document; Technical Characteristics of Multiple Gigabit Wireless System in the 60 GHz Range. ETSI DTR/ERM-RM-049, 2006.

[12] [Online]. Available: http://www.chinabwips.org/index.htm

[13] in *Proc. Korean Frequency Policy and Technology Workshop, Session 7*, Nov. 2005, pp. 13–32.

[14] [Online]. Available: http://www.ieee802.org/15/pub/TG3c.html

[15] A. Sadri, "802.15.3c usage model document," IEEE 802.15-06-0055-14-003c, May 2006.

[16] R. C. Daniels and R. W. Heath, "60 GHz wireless communications: Emerging requirements and design recommendations," *IEEE Veh. Technol. Mag.*, vol. 2, no. 3, pp. 41–50, Sep. 2007.

[17] S. K. Yong and C. C. Chong, "An overview of multigigabit wireless through millimeter wave technology: potentials and technical challenges," *EURASIP J. Wireless Commun. Networking*, 2007, Article ID: 78907.

[18] K. Ohata *et al.*, "1.25 Gbps wireless Gigabit Ethernet link at 60 GHz-band," in *IEEE MTT-S Int. Microwave Symp. Dig.*, Philadelphia, PA, Jun. 8-13, 2003, pp. 373–376.

[19] S. E. Gunnarsson *et al.*, "Highly integrated 60 GHz transmitter and receiver MMICs in a GaAs pHEMT technology," *IEEE J. Solid-State Circuits*, vol. 40, no. 11, pp. 2174–2186, Nov. 2005.

[20] S. E. Gunnarsson *et al.*, "60 GHz single-chip front-end MMICs and systems for multi-Gb/s wireless communication," *IEEE J. Solid-State Circuits*, vol. 42, no. 5, pp. 1143–1157, May 2007.

[21] B. Floyd, S. Reynolds, U. Pfeiffer, T. Beukema, J. Grzyp, and C. Haymes, "A silicon 60 GHz receiver and transmitter chipset for broadband communications," in *IEEE ISSCC Dig.*, San Francisco, CA, Feb. 4-9, 2006, pp. 184–185.

[22] C. H. Wang *et al.*, "A 60 GHz transmitter with integrated antenna in 0.18 um SiGe BiCMOS technology," in *Proc. IEEE ISSCC Dig.*, San Francisco, CA, Feb. 5-9, 2006, pp. 186–187.

[23] B. Razavi, "CMOS transceiver for the 60-GHz band," in *Proc. IEEE RFIC* , San Francisco, CA, Jun. 11-13, 2006, p. 4.

[24] D. Huang, R. Wong, Q. Gu, N. Y. Wang, T. W. Ku, C. Chien, and M. -C. F. Chang, "A 60 GHz CMOS differential receiver front-end using on-chip transformer for 1.2 volt operation with enhanced gain and linearity," in *Proc. Symp. VLSI Circuits*, Honolulu, HI, Jun. 15-17, 2006, pp. 144–145.

[25] M. Toshiya *et al.*, "A 60-GHz CMOS receiver with frequency synthesizer," in *IEEE Symp. VLSI Dig.*, Kyoto, Japan, Jun. 14-16, 2007, pp. 172–173.

[26] S. Pinel, S. Sarkar, P. Sen, B. Perumana, D. Yeh, D. Dawn, and J. Laskar, "A 90 nm CMOS 60 GHz radio," in *IEEE ISSCC Dig.*, San Francisco, CA, Feb. 5-9, 2008, pp. 186–187.

[27] D. Alldred, B. Cousins, and S. P. Voinigescu, "A 1.2 V, 60-GHz radio receiver with on-chip transformers and inductors in 90-nm CMOS," in *Proc. IEEE Compound Semiconductor Integrated Circuits Symp.*, San Antonio, TX, Nov. 12-15, 2006, pp. 144–145.

[28] A. Parsa and B. Razavi, "A 60 GHz receiver using a 30 GHz LO," in *IEEE ISSCC Dig.*, San Francisco, CA, Feb. 5-9, 2008, pp. 186–187.

[29] B. Afshar, Y. Wang, and A. Niknejad, "A robust 24 mW 60 GHz receiver in 90 nm standard CMOS," in *IEEE ISSCC Dig.*, San Francisco, CA, Feb. 5-9, 2008, pp. 186–187.

[30] M. Varonen, M. Kärkkäinen, and K. A. I. Halonen, "Millimeter-wave amplifiers in 65-nm CMOS," in *Proc. ESSCIRC*, Munich, Germany, Sep. 10-14, 2007, pp. 280–283.

[31] T. Manabe, Y. Miura, and T. Ihara, "Effects of antenna directivity and polarization indoor multipath propagation characteristics at 60 GHz," *IEEE J. Sel. Areas Commun.*, vol. 14, pp. 441–448, Apr. 1996.

[32] H. B. Yang, P. F. M. Smulders, and M. H. A. J. Herben, "Channel characteristics and transmission performance for various channel configurations at 60 GHz," *EURASIP J. Wireless Commun. Networking*, 2007, Article ID: 19613.

[33] E. Grass, F. Herzel, M. Piz, Y. Sun, and R. Kraemer, "Implementation aspects of Gbit/s communication system for 60 GHz band," in *Proc. 14th Wireless World Research Forum*, San Diego, CA, Jun. 29-30, 2005, pp. 1–8.

[34] R. B. Dybdal, "Millimeter wave antenna technology," *IEEE J. Sel. Areas Commun.*, vol. 1, no. 4, pp. 633–644, Sep. 1983.

[35] [Online]. Available: http://www.ist-broadway.org/documents/deliverables/broadway-wp4-d10.pdf

[36] S. Collonge, G. Zaharia, and G. E. Zein, "Influence of human activity on wideband characteristics of the 60 GHz indoor radio channel," *IEEE Trans. Wireless Commun.*, vol. 3, no. 6, pp. 2396–2406, 2004.

[37] J. G. Kim, H. S. Lee, H. Lee, J. B. Yoon, and S. Hong, "60-GHz CPW-fed post-supported patch antenna using micromachining technology," *IEEE Microw. Wireless Compon. Lett.*, vol. 15, no. 10, pp. 635–637, Oct. 2005.

[38] H. Uchimura, N. Shino, and K. Miyazato, "Novel circular polarized antenna array substrates for 60 GHz-band," in *IEEE MTT-S Int. Microwave Symp. Dig.*, Long Beach, CA, Jun. 12-17, 2005, pp. 1875–1878.

[39] I. I. Kim, S. Pinel, J. Laskar, and J. G. Yook, "Circularly & linearly polarized fan beam patch antenna arrays on liquid crystal polymer substrate for V-band applications," in *Asia-Pacific Microwave Conf. Proc.*, Suzhou, Jiangsu, China, Dec. 4-7, 2005, vol. 4.

[40] C. Karnfelt, P. Hallbjorner, H. Zirath, and A. Alping, "High gain active microstrip antenna for 60-GHz WLAN/WPAN applications," *IEEE Trans. Microw. Theory Tech.*, vol. 54, no. 6, pp. 2593–2603, Jun. 2006.
[41] A. Babakhani, X. Guan, A. Komijani, A. Natarajan, and A. Hajimiri, "A 77-GHz phased-array transceiver with on-chip antennas in silicon: receiver and antennas," *IEEE J. Solid-State Circuits*, vol. 41, no. 12, pp. 2795–2806, Dec. 2006.
[42] Y. P. Zhang, L. H. Guo, and M. Sun, "On-chip antennas for 60-GHz radios in silicon technology," *IEEE Trans. Electron Devices*, vol. 52, no. 7, pp. 1664–1668, Jul. 2005.
[43] K. T. Chan *et al.*, "Integrated antennas on Si with over 100 GHz performance, fabricated using an optimized proton implantation process," *IEEE Microw. Wireless Compon. Lett.*, vol. 13, no. 11, pp. 487–489, Nov. 2003.
[44] H. R. Chuang, S. W. Kuo, C. C. Lin, and L. C. Kuo, "A 60-GHz millimeter-wave CMOS RFIC-on-chip dipole antenna," *Microw. J.*, vol. 50, no. 1, p. 144, Jan. 2007.
[45] C. S. Wang, J. W. Huang, S. H. Wen, S. H. Yeh, and C. K. Wang, "A CMOS RF front-end with on-chip antenna for V-band broadband wireless communications," in *Proc. ESSCIRC*, Munich, Germany, Sep. 10-14, 2007, pp. 143–146.
[46] M. A. T. Sanduleanu, "60 GHz integrated circuits and wireless systems," presented at the ESSCIRC, Munich, Germany, Sep. 18-22, 2006.
[47] [Online]. Available: http://www.signal.uu.se/Publications/abstracts/a061.html
[48] H. S. Pisheh, Y. Komijany, M. Shahabadi, S. Mohajerzadeh, and M. Araghchini, "Design, simulation, and fabrication of a novel multi-band miniaturized antenna for wireless communication applications," in *Proc. 30th Int. Conf. Infrared and Millimeter Waves*, Williamsburg, VA, Sep. 19-23, 2005, pp. 551–552.
[49] K. K. O *et al.*, "On-chip antennas in silicon ICs and their applications," *IEEE Trans. Electron Devices*, vol. 52, no. 7, pp. 1312–1323, Jul. 2005.
[50] M. R. N. Ahmadi, S. N. Safieddin, and L. Zhu, "On-chip antennas for 24, 60, and 77 GHz single package transceivers on low resistivity silicon substrate," in *Proc. IEEE Antenna Propag. Symp.*, Honolulu, HI, Jun. 10-15, 2007, pp. 5059–5062.
[51] U. Pfeiffer, J. Grzyp, D. Liu, B. Gaucher, T. Beukema, B. Floyd, and S. Reynolds, "A chip-scale packaging technology for 60-GHz wireless chipsets," *IEEE Trans. Microw. Theory Tech.*, vol. 54, no. 8, pp. 3387–3397, Aug. 2006.
[52] U. Pfeiffer, J. Grzyp, D. Liu, B. Gaucher, T. Beukema, B. Floyd, and S. Reynolds, "A 60-GHz radio chipset fully-integrated in a low-cost packaging technology," in *Proc. 56th Electron. Compon. Technol. Conf.*, San Diego, CA, Jun. 2, 2006, pp. 1343–1346.
[53] T. Zwick, D. Liu, and B. Gaucher, "Broadband planar superstrate antenna for integrated millimeter-wave transceivers," *IEEE Trans. Antennas Propag.*, vol. 54, no. 10, pp. 270–2796, Oct. 2006.
[54] D. Liu and B. Gaucher, "Design consideration for millimetre wave antennas within a chip package," in *Proc. IEEE Int. Workshop Antenna Technol.*, Xiamen, China, Apr. 21-23, 2007, pp. 13–16.
[55] Y. Tsutsumi *et al.*, "A triangular loop antenna mounted adjacent to a lossy Si substrate for millimeter-wave wireless PAN," in *Proc. IEEE Antennas Propag. Symp.*, Honolulu, HI, Jun. 10-15, 2007, pp. 1008–1011.
[56] T. Seki, K. Nishikawa, I. Toyoda, and K. Tsunekawa, "Millimeter-wave high-efficiency multilayer parasitic microstrip antenna array for system-on-package," *NTT Tech. Rev.*, vol. 3, no. 9, pp. 33–40, Sep. 2005.
[57] Y. C. Lee, W. Chang, and C. S. Park, "Monolithic LTCC SiP transmitter for 60 GHz wireless communication terminals," in *IEEE MTT-S Int. Microwave Symp. Dig.*, Long Beach, CA, Jun. 12-17, 2005, pp. 1015–1018.
[58] L. Desclos, "V-band double slot antenna integration on LTCC substrate using thick film technology," *Microw. Opt. Technol. Lett*, vol. 28, no. 5, pp. 354–357, Mar. 2001.
[59] Y. P. Zhang, M. Sun, K. M. Chua, L. L. Wai, D. Liu, and B. Gaucher, "Antenna-in-package in LTCC for 60-GHz radio," in *Proc. IEEE Int. Workshop Antenna Technol.*, Cambridge, U.K., Mar. 21-23, 2007, pp. 279–282.
[60] N. H. Hoivic *et al.*, "High-efficiency 60 GHz antenna fabricated using low-cost silicon micromachining techniques," in *Proc. IEEE Antennas Propag. Symp.*, Honolulu, HI, Jun. 10-15, 2007, pp. 5043–5046.
[61] Y. J. Yoon and B. Kim, "A new formula for effective dielectric constant in multi-dielectric layer microstrip structure," in *Proc. IEEE Electrical Perform. Electronic Packag.*, Scottsdale, AZ, Oct. 23-25, 2000, pp. 163–167.
[62] N. G. Alexopoulos, P. B. Katehi, and D. B. Rutledge, "Substrate optimization for integrated circuit antennas," *IEEE Trans. Microw. Theory Tech.*, vol. 31, no. 7, pp. 550–557, Jul. 1983.
[63] Y. P. Zhang, Y. Hwang, and G. X. Zheng, "A gain-enhanced probe-fed microstrip antenna of very high permittivity," *Microw. Opt. Technol. Lett.*, vol. 15, pp. 89–91, 1997.
[64] [Online]. Available: http://etd.gatech.edu/theses/available/etd-04072006-151337/unrestricted/thompson_dane_c_200605_phd.pdf
[65] [Online]. Available: http://www.ltcc.de/en/home.phpSIMT
[66] [Online]. Available: http://www.vtt.fi
[67] [Online]. Available: http://www.simtech.a-star.edu.sg/
[68] R. H. Caverly, "Characteristic impedance of integrated circuit bond wires," *IEEE Trans. Microw. Theory Tech.*, vol. 34, no. 9, pp. 982–984, Sep. 1986.
[69] G. Baumann *et al.*, "51 GHz frontend with flip chip and wire bond interconnections from GaAs MMICs to a planar patch antenna," in *IEEE MTT-S Int. Microwave Symp. Dig.*, Orlando, FL, May 16-20, 1995, pp. 1639–1642.
[70] T. Krems, W. Haydl, H. Massler, and J. Rudiger, "Millimeter-wave performance of chip interconnections using wire bonding and flip chip," in *IEEE MTT-S Int. Microwave Symp. Dig.*, San Francisco, CA, Jun. 17-21, 1996, pp. 247–250.
[71] Y. Sun, S. Glisic, F. Herzel, K. Schmalz, E. Grass, W. Winkler, and R. Kraemer, "An integrated 60 GHz transceiver front end for OFDM in SiGe: BiCMOS," presented at the Wireless World Research Forum 16, Shanghai, China, Apr. 26-28, 2006.
[72] Y. P. Zhang, M. Sun, K. M. Chua, L. L. Wai, and D. Liu, "Antenna-in-package design for wirebond interconnection to highly-integrated 60-GHz radios," *IEEE Trans. Antennas Propagat.*, vol. 57, no. 10, Oct. 2009.
[73] Y. P. Zhang, "Enhancement of package antenna approach with dual feeds, guard ring, and fence of vias," *IEEE Trans. Adv. Packag.*, vol. 32, no. 3, pp. 612–618, Aug. 2009.

Y. P. Zhang received the B.E. and M.E. degrees from Taiyuan Polytechnic Institute and Shanxi Mining Institute of Taiyuan University of Technology, Shanxi, China, in 1982 and 1987, respectively, and the Ph.D. degree from the Chinese University of Hong Kong, Hong Kong, in 1995, all in electronic engineering.

From 1982 to 1984, he worked at Shanxi Electronic Industry Bureau, from 1990 to 1992, the University of Liverpool, Liverpool, U.K., and from 1996 to 1997, City University of Hong Kong. From 1987 to 1990, he taught at Shanxi Mining Institute and from 1997 to 1998, the University of Hong Kong. He was promoted to a Full Professor at Taiyuan University of Technology in 1996. He is now an Associate Professor and the Deputy Supervisor of Integrated Circuits and Systems Laboratories with the School of Electrical and Electronic Engineering, Nanyang Technological University, Singapore. He has broad interests in radio science and technology and has published widely across seven IEEE societies. He has delivered scores of invited papers/keynote addresses at international scientific conferences.

Prof. Zhang received the Sino-British Technical Collaboration Award in 1990 for his contribution to the advancement of subsurface radio science and technology. He received the Best Paper Award from the Second IEEE International Symposium on Communication Systems, Networks and Digital Signal Processing, 18–20 July 2000, Bournemouth, U.K., and the Best Paper Prize from the Third IEEE International Workshop on Antenna Technology, 21–23 March 2007, Cambridge, U.K. He was awarded a William Mong Visiting Fellowship from the University of Hong Kong in 2005. He is listed in *Marquis Who's Who, Who's Who in Science and Engineering, Cambridge IBC 2000 Outstanding Scientists of the 21st Century.* He serves on the Editorial Board of the *International Journal of RF and Microwave Computer-Aided Engineering and* was a Guest Editor of the *Journal* for the special issue *RF and Microwave Subsystem Modules for Wireless Communications*. He also serves as an Editor of *ETRI Journal*, an Associate Editor of the *International Journal of Microwave Science and Technology* and an Associate Editor of the *International Journal of Electromagnetic Waves and Applications*. Furthermore, he serves on the

Editorial Boards of IEEE TRANSACTIONS ON MICROWAVE THEORY AND TECHNIQUES and *IEEE Microwave and Wireless Components Letters*.

Duixian Liu (S'85-M'90-SM'98) received the B.S. degree in electrical engineering from XiDian University, Xi'an, China, in 1982, and the M.S. and Ph.D. degrees in electrical engineering from the Ohio State University, Columbus, in 1986 and 1990, respectively.

From 1990 to 1996, he was with Valor Enterprises Inc. Piqua, Ohio, initially as an Electrical Engineer and then as the Chief Engineer, during which time he designed an antenna product line ranging from 3 MHz to 2.4 GHz for the company, a very important factor for the prestigious Presidential "E" Award for Excellence in Exporting in 1994. Since April 1996, he has been with the IBM T. J. Watson Research Center, Yorktown Heights, NY, as a Research Staff Member. He has authored or coauthored approximately 60 journal and conference papers. He has 28 patents issued and 15 patents pending. He has served as external Ph.D. examiner for several universities and external examiner for some government organizations on research grants. His research interests are antenna design, EM modeling, chip packaging, electromagnetic modeling, digital signal processing, and communications technology.

Dr. Liu has received three IBM Outstanding Technical Achievement Awards and one Corporate Award, the IBM's highest technical award. He was named Master Inventor in 2007. He is an Associate Editor for the IEEE TRANSACTIONS ON ANTENNAS AND PROPAGATION and a Guest Editor for the current IEEE TRANSACTIONS ON ANTENNAS AND PROPAGATION Special Section on Antennas and Propagation Aspects of 60–90 GHz Wireless Communications. He has been the organizer or chair for numerous international conference sessions or special sessions and also a technical program committee member. He was the general chair of the 2006 IEEE International Workshop on Antenna Technology: Small Antennas and Novel Metamaterials, White Plains, New York.